Biogeosciences Discuss., https://doi.org/10.5194/bg-2017-329
Manuscript under review for journal Biogeosciences
Discussion started: 4 September 2017

Smaller global and regional carbon emissions from gross land use change when considering sub-grid secondary land cohorts in a global dynamic vegetation model

Chao Yue, Philippe Ciais, Wei Li

Laboratoire des Sciences du Climat et de l'Environnement, LSCE/IPSL, CEA-CNRS-UVSQ, Université Paris-Saclay, F-91191 Gif-sur-Yvette, France

Corresponding author: Chao Yue, chao.yue@lsce.ipsl.fr

Running title: Lower gross land use carbon emissions

Abstract

Several modeling studies reported elevated carbon emissions from historical land use change (LUC) by including bi-directional transitions at the sub-grid scale (termed gross land use change). This has implication on the estimation of so-called residual land CO_2 sink over undisturbed lands. However, in most dynamic global vegetation models (DGVM), forests and/or other land use types are represented with a single sub-grid tile, without accounting for secondary lands that are often involved in shifting cultivation or wood harvest. As a result, land use change emissions (E_{LUC}) are likely overestimated, because it is high-biomass mature forests instead of low-biomass secondary forests that are cleared. Here we investigated the effects of including sub-grid forest age dynamics in a DGVM on historical E_{LUC} over 1501–2005. We run two simulations, one with no forest age ($S_{ageless}$) and the other with sub-grid secondary forests of different age classes whose demography is driven by historical land use change (S_{age}). Estimated global E_{LUC} for 1501–2005 are 179 Pg C in S_{age} compared to 199 Pg C in $S_{ageless}$. The lower emissions in S_{age} arise mainly from shifting cultivation in the tropics, being of 27 Pg C in S_{age} against 46 Pg C in $S_{ageless}$. Estimated cumulative E_{LUC} from wood harvest in the S_{age} simulation (31 Pg C) are however slightly higher than $S_{ageless}$ (27 Pg C), because secondary forests simulated in S_{age} are insufficient to meet the prescribed harvest area, leading to the harvest of old forests. This result depends on pre-defined forest clearing priority rules given a simulated portfolio of differently aged forests in the model. Our results highlight that although gross land use change as a former missing emission component is included by a growing number of DGVMs, its contribution to overall E_{LUC} tends to be overestimated, unless low-biomass secondary forests are properly represented.

Keywords: gross land use change, carbon emission, secondary forests, shifting cultivation, wood harvest.

Biogeosciences Discuss., https://doi.org/10.5194/bg-2017-329
Manuscript under review for journal Biogeosciences
Discussion started: 4 September 2017

35

36 **Nomenclature**

37 LUC : land use change

38 E_{LUC} : carbon emissions from land use change. Positive values indicate that LUC has a net effect of
39 releasing carbon from vegetation to the atmosphere, while a negative value indicates the reverse, i.e.,
40 carbon is uptaken from the atmosphere to vegetation.

41 $E_{LUC\ process[,\ configuration]}$: carbon emissions from a certain LUC *process* (***net*** *transitions only, land* ***turnover****,*
42 *wood* ***harvest*** or ***all*** *three processes combined*) quantified by a specific model *configuration* (***age*** or
43 ***ageless***, in which differently aged sub-grid land cohorts are, or are not explicitly represented,
44 respectively). For instance, $E_{LUC\ net,\ ageless}$ indicates E_{LUC} from net transitions only as simulated by model
45 runs that do not explicitly represent sub-grid age dynamics, i.e., a single ageless mature patch is used to
46 represent a land cover type; $E_{LUC\ net,\ age}$ indicates E_{LUC} from the same process using a model configuration
47 that explicitly represents differently aged land cohorts since their establishment.

48 S_{age}: Model simulations that represents sub-grid secondary land cohorts since their establishment.

49 $S_{ageless}$: Model simulations that do not include sub-grid age dynamics, i.e., a single ageless mature patch is
50 used to represent a land cover type.

51

52 **1 Introduction**

53 Historical land use change (LUC), such as the permanent establishment of agricultural land on forests, or
54 shifting cultivation or wood harvest, has contributed significantly to the atmospheric CO_2 increase, in
55 particular since industrialization (Houghton, 2003; Le Quéré et al., 2016; Pongratz et al., 2009). Carbon
56 emissions from land use change (E_{LUC}) are often defined as a net effect of carbon release from newly
57 disturbed lands, given that in most cases newly created lands have a lower carbon density than primary
58 ecosystems (e.g., forest to cropland), and carbon uptake by some recovering ecosystems (e.g., cropland
59 abandonment). As the high spatial heterogeneity of land conversions prohibits any direct measurement of
60 global or regional E_{LUC}, modeling turned out to be the only approach to its quantification (Gasser and
61 Ciais, 2013; Hansis et al., 2015; Houghton, 1999, 2003; Piao et al., 2009). Methods to quantify E_{LUC}
62 could fall broadly into three categories, namely bookkeeping models (Gasser and Ciais, 2013; Hansis et
63 al., 2015; Houghton, 2003), dynamic global vegetation models (Shevliakova et al., 2009; Stocker et al.,
64 2014; Wilkenskjeld et al., 2014; Yang et al., 2010), and fire-based estimates of deforestation fluxes (van
65 der Werf et al., 2010).

66

67 Despite a plethora of studies trying to quantify historical LUC emissions (Hansis et al., 2015; Houghton
68 et al., 2012; Stocker et al., 2014; Wilkenskjeld et al., 2014), it remains the least constrained term in the

global carbon budget, estimated to be 1.0 Pg C yr^{-1} for the last decade with an uncertainty of 0.5 Pg C yr^{-1} (Le Quéré et al., 2016). The large spread of modeled LUC emissions (e.g., Fig. 1 in Houghton et al., 2012) arises from a wide range of factors, including terminological inconsistencies (Pongratz et al., 2014; Stocker and Joos, 2015), different approaches to implement LUC processes in models (e.g., net LUC as a net change between two consecutive snapshots of land cover maps, versus gross LUC in which sub-grid bi-directional transitions between two land cover types is accounted for, see discussions in Prestele et al., 2016); whether agricultural land is converted from former forested land or grassland, see discussions in Peng et al., 2017), different model processes (e.g., with nitrogen cycle or not, see discussions in Jain et al., 2013) or different initial carbon pools prior to LUC activities (Li et al., 2017).

When including sub-grid scale bi-directional gross land use changes such as shifting cultivation or other forms of land turnover processes, models are found to yield higher estimates of E_{LUC} for 1850-2005 ranging 2-38% depending on different models and assumptions than accounting for net transitions only. Wood harvest, although it does not change the underlying land cover type, can also lead to additional carbon emissions due to the fast carbon release from recently harvested forests and slow uptake from re-growing ones (Shevliakova et al., 2009; Stocker et al., 2014). Recently, both gross land use change and forest wood harvest have been included in some of the bookkeeping models (Hansis et al., 2015; Houghton, 2003) and in dynamic global vegetation models as well (Shevliakova et al., 2009; Stocker et al., 2014). But their inclusion remain a task to do for many other DGVMs: for instance, none of the vegetation models used in the Global Carbon Project (GCP) annual budget has included shifting cultivation and only a few included wood harvest (Le Quéré et al., 2016).

While replacing forest with cropland or pasture typically leads to carbon release, forest restoration and abandonment of previously cultivated land or afforestation typically sequester carbon in growing biomass stocks. Some recent studies, both at site (Poorter et al., 2016) and regional scales (Chazdon et al., 2016), show that secondary forests currently recovering from historical land use change have are contributing to terrestrial carbon uptake, and that the carbon stored per unit land sometimes exceeds that of the original primary forest (Poorter et al., 2016). While explicit representing secondary land cohorts with different time lengths since the last disturbance is relatively straightforward in bookkeeping models thanks to their light demand in computation (Hansis et al., 2015), it remains rarely implemented for large-scale vegetation models (exceptions are Shevliakova et al., 2009; Stocker et al., 2014; Yang et al., 2010) with only a single group of secondary land being implemented in the latter two cases). Instead, forest or other land cover types are, in most cases, represented as a single mature ageless patch in each grid cell. This tends to overestimate carbon emissions from shifting cultivation or wood harvest, in case a stable rotation

cycle is established in these practices and low-biomass secondary forest is targeted for clearance, as shown in (Yue et al., 2017).

In this study, we quantify global and regional carbon emissions from historical gross land use change since 1501 using a global vegetation model ORCHIDEE (ORganizing Carbon and Hydrology In Dynamic EcosystEms) that has recently incorporated the representation of sub-grid secondary land cohorts of different age classes. Our objectives are: 1) to quantify carbon emissions from historical gross land use change since 1501 and compare them with previous studies, and to examine the impacts on E_{LUC} when considering sub-grid secondary land cohorts by using parallel model simulations with and without sub-grid secondary land cohorts. 2) Examine contributions to E_{LUC} from different LUC processes (i.e., net transitions only, shifting cultivation or land turnover, and wood harvest) and how they differ between the two model configurations with and without secondary land cohorts.

2 Methods

2.1 ORCHIDEE-MICT-GLUC model and the implemented gross land use change processes

ORCHIDEE (Krinner et al., 2005) is a dynamic global vegetation model (DGVM) and the land surface component of the IPSL Earth System Model (ESM). It comprises three sub-models operating on different time steps. SECHIBA operates on half-hourly time step and simulates fast exchanges in energy, water and momentum between vegetation and the atmosphere. STOMATE operates on daily time step and simulates vegetation carbon cycle processes including photosynthate allocation, plant phenology, vegetation mortality and recruitment. The third sub-model contains various modules about different processes on varying time steps, such as vegetation dynamics (daily), fire disturbance (daily), and land use change (annual time step).

The land use change module originally contained in ORCHIDEE was developed in Piao *et al*. (2009) where only net transitions are taken into account. Recently, gross land use change and explicit representation of differently aged sub-grid land cohorts have been developed in a branch of ORCHIDEE model known as ORCHIDEE-MICT (Guimberteau et al., 2017). This model will be henceforth referred to as ORCHIDEE-MICT-GLUC (Yue et al., 2017). Idealized site-scale simulations with this model have shown that estimated carbon emissions from shifting cultivation and wood harvest are reduced by explicitly including sub-grid age dynamics, in comparison with an alternative approach to representing land cover types with a single ageless patch. This is because the secondary forests that are cleared in a rotational practice of shifting cultivation or forestry (wood harvest) have lower biomass than the forests in the ageless parameterization, which have carbon stocks close to mature forests. Yue et al. (2017) provide

details on the processes involved in explaining differences in E_{LUC} regarding whether forest age is considered or not.

The gross land use change module in ORCHIDEE-MICT-GLUC operates on an annual time step. For the very first year of the simulation, an initial land cover map (represented as a map of plant function types or PFTs) is prescribed. Land cover maps of following years are updated annually using land use transition matrices corresponding to LUC processes. Land use transitions among four vegetated land cover types are included: forest, natural grassland, pasture and cropland. The model separates overall LUC into three additive sub-processes in order to diagnose their individual contributions to E_{LUC}, namely net land use change equivalent to the original approach that considers net transitions only, land turnover equivalent to shifting cultivation, and wood harvest. Matrices for net land use change and land turnover ($[X_{i,j}]$) take the form of 4 rows by 4 columns, with $X_{i,j}$ indicating the land transition from vegetation type i to j. The matrix for wood harvest has only two elements, indicating ground fractions of forest subject to harvest from primary and secondary forests, respectively. The current model version assumes that bare land fraction remains constant throughout the entire simulation.

As is mentioned above, ORCHIDEE-MICT-GLUC is capable of representing sub-grid secondary even-aged land cohorts (named age classes), expressed to have different time lengths since their establishment. Differentiation of age classes applies on all vegetation types in the model. The number of age classes for each PFT can be customized via a configuration file. Age classes for forest PFTs are distinguished in terms of woody biomass, while those for herbaceous PFTs are defined using soil carbon stock. Newly transitioned land is assigned to the youngest age class. Forest cohorts will move to the next age class when their woody biomass exceeds the threshold during forest growth. For herbaceous PFTs, younger age classes are parameterized to have a smaller soil carbon stock, to reflect the typical case where soil carbon degrades when croplands are created from forests (e.g., Don et al., 2011; Poeplau et al., 2011). Hence with the degradation of legacy soil carbon stock, herbaceous cohorts will move into next age class.

To simulate land use change when taking into account sub-grid land cohorts, a set of priority rules become necessary regarding which land cohorts to target given a specific LUC type, and how to allocate LUC area into different PFTs of the same age class. For net land use change, clearing of forests exclusively starts from the oldest cohorts and then moves onto younger ones until the youngest ones. For shifting cultivation or land turnover, forest clearing starts from a pre-defined middle-aged class, and then moves onto older ones if this starting age class is used up, until the oldest ones. This is to accommodate the assumption used in the LUC forcing data that shifting cultivation has a certain residence time (see the

171 next section), so that secondary forests are given a high priority to be cleared for agricultural land, and
172 older forests will be cleared when even more agricultural lands are needed. Forest wood harvest follows
173 the same rule as shifting cultivation regarding on which forest cohorts to clear. Finally, for all other land
174 cover types that are used as a source for conversion, we start from the oldest age class and move
175 sequentially to younger ones, in order to meet the prescribed LUC area in the forcing data. After the LUC
176 area is allocated on the cohort (age class) level, it is then distributed among different PFTs in proportion
177 to their existing areas in this cohort.
178
179 In order to compare the simulated LUC impacts with and without sub-grid secondary land cohorts,
180 ORCHIDEE-MICT-GLUC can be run in a way that each PFT has only one single age class. This is
181 equivalent to the alternative approach by which no sub-grid land cohorts are simulated, i.e., the traditional
182 approach with a single ageless patch for each vegetation type. For more information on the rationale and
183 details of LUC implementation in ORCHIDEE-MICT-GLUC, readers are referred to Yue et al. (2017).
184
185 **2.2 Preparation of forcing land use change matrices**
186 For historical land use transitions, the land use harmonized data set version 1 (LUH1) for the CMIP5
187 project was used (Hurtt et al., 2011, http://luh.umd.edu/data.shtml#LUH1_Data). We used the version of
188 LUH1 data without urban land as ORCHIDEE-MICT-GLUC does not simulate the effects of urban
189 lands.The original data set is at 0.5° spatial resolution with an annual time step covering 1500-2005. Four
190 land use types are included: primary natural land, secondary natural land, pasture and cropland. The type
191 of "natural land" implicitly consists of grassland and forest (which are separated in ORCHIDEE-MICT-
192 GLUC) but their relative fractions are not separated. In LUH1, land use transitions from either primary or
193 secondary natural land to pasture or cropland are provided, and vice versa. Secondary natural lands
194 originated from pasture or cropland abandonment. Besides, land use transitions between pasture and
195 cropland are provided as well. Harvested wood comes either from primary or secondary forest, with
196 ground area fractions that are harvested being available. Note that this does not contradict with the fact
197 that forest and grassland fractions are not separated within the land use type of "natural land", because
198 forests are defined as natural lands with a certain biomass carbon, which is further simulated by a
199 terrestrial model (Hurtt et al., 2006).
200
201 Rather than the simple terrestrial model (Miami-LU) used in Hurtt et al. (2011) to separate natural
202 vegetation into forested and non-forest land, ORCHIDEE-MICT-GLUC distinguishes 8 forest PFTs, 2
203 natural grassland PFTs, 2 cropland PFTs (Krinner et al., 2005) and 2 additional pasture PFTs. Thus, to
204 use LUH1 historical LUC transition reconstructions as a forcing input, assumptions have to be made to

disaggregate LUH1 land use types into corresponding PFTs in the model. For this purpose, we used an ORCHIDEE-compatible PFT map generated from the European Space Agency (ESA) Climate Change Initiative (CCI) land cover map covering a 5-year period of 2003-2007 (European Space Agency, 2014), assuming that it corresponds to the land use distribution for 2005 by the LUH1 data. Subsequently, we backcast historical PFT map time series for 1500-2004 based on this 2005 PFT map using LUH1 historical net land use transitions as a constraint. Because land turnover involves an equal, bi-directional land transition between two land cover types, it does not lead to any net change in the PFT map. Therefore, only net transition information is needed when backcasting historical PFT maps.
The guiding principle of backcasting is that when ORCHIDEE is forced by historical net land cover matrices (as constrained by the LUH1 data) starting from the year 1500, it should reach exactly the PFT map in 2005 based on ESA CCI land cover map. To separate land use transitions in LUH1 into processes of net land use change and land turnover, we simply treat the minimum reverse fluxes between two land use types as the land turnover, and the remaining as net land use change. During the backcasting process, reconciliations have to be made where LUH1 data disagrees with the ESA map at the grid cell scale.

When backcasting historical PFT map time series using net land use change matrices, we assume that when pasture or cropland is created, they come from an equal share of forest and grassland; when their fractions decrease, cropland abandonment leads first to forest recovery and then followed by grassland, while pasture abandonment leads to an equal share of forest and natural grassland expansion. For each year, the land turnover transition between two land use types is not allowed to exceed the minimum of their existing areas. Spatially resolved forest harvest time series are provided in LUH1. We built the wood harvest matrices by limiting wood harvest area within the total area of forest PFTs over each grid cell for each year. For more details on PFT map backcasting and the construction of land use transition matrices, readers are referred to the Supplement Material.

The construction of historical PFT maps and land transition matrices was done at 2° resolution for the whole globe, after re-sampling all input data from their original resolution to 2°. The reconstructed global forest area agrees with that by Peng et al. (2017), who has backcast historical ORCHIDEE PFT map series using the same ESA CCI 2005 PFT map and historical pasture and crop distributions from LUH1 but not the LUH1 land use transitions, with historical forest areas in the nine regions of the globe being constrained by data in Houghton (2003) based on national forest area statistics. The land turnover transitions between secondary land (forest and grassland) and cropland (or pasture) from the matrices defined above are slightly smaller than originally prescribed in LUH1, because some of the prescribed transitions are ignored due to the inconsistency between LUH1 map in 2005 and the 2005 PFT map based

on ESA CCI land cover map (See Supplement Material for detailed comparison). Note that shifting cultivation (land turnover) is limited within the tropical regions as in LUH1, and the land turnover resulting from the upscaling of 0.5° to 2° is not included.

2.3 Simulation protocol

2.3.1 Separate contributions of different land use change processes

The PFT map of year 1500 as generated from the backcasting procedure (see the previous section) was used during the model spin-up. Climate data used were CRUNCEP v5.3.2 climate forcing at 2° resolution covering 1901-2013 (https://vesg.ipsl.upmc.fr/thredds/fileServer/store/p529viov/cruncep/readme.html). For the spin-up, climate data were cycled from 1901 to 1910, with atmospheric CO_2 concentration being fixed at the 1750 level (277 ppm). Following LUH1 (Hurtt et al., 2011), we assume that no land use change occurs during the model spin-up. The spin-up lasts for 450 years and includes a specific accelerated soil carbon module to speed up the equilibrium of soil carbon stock. Fires and fire carbon emissions are simulated with a prognostic fire module (Yue et al., 2014), with fire occurring only on forests and natural grasslands. Simulated net land-atmosphere carbon flux is calculated as net biome production (NBP):

$$NBP = NPP - F_{Inst} - F_{Wood} - F_{HR} - F_{Fire} - F_{AH} - F_{pasture} \quad \text{Eq (1)}$$

Where NPP is the net primary production. All fluxes starting with "F" are outward fluxes (i.e., carbon source from the ecosystem perspective), with F_{Inst} being instantaneous carbon fluxes lost during LUC (e.g., site preparation, deforestation fires etc.), F_{Wood} for delayed carbon emissions from the degradation of harvested wood product pools, F_{HR} for soil respiration, F_{AH} for carbon emissions from agricultural harvest, including harvest from croplands and pastures (treated as a carbon source for the year of harvest equaling the harvested biomass; this source is assumed to occur on the grid cell harvested, ignoring the transport, processing and final consumption of agricultural yield), and $F_{pasture}$ for additional non-harvest carbon sources from pastures including export of animal milk and methane emissions. Carbon emissions from land use change (E_{LUC}) are quantified as the differences in NBP between simulations without and with LUC, with positive values representing carbon sources (i.e., LUC emissions). We conducted a set of additive factorial simulations by including matrices of different LUC processes in each simulation (Table 1), which allow quantifying E_{LUC} from different LUC processes. Henceforth for briefness, we denote the simulation without sub-grid age class dynamics as $S_{ageless}$, simulation with sub-grid age dynamics as S_{age}.

2.3.2 Define thresholds for age classes

Biogeosciences Discuss., https://doi.org/10.5194/bg-2017-329
Manuscript under review for journal Biogeosciences
Discussion started: 4 September 2017

For the simulation with age dynamics (S_{age}), six age classes are used for forest PFTs and two age classes for other PFTs. As explained, age classes of forest PFTs are separated in terms of woody biomass. The LUH1 data assumes a 15-year residence time for agricultural land in shifting cultivation in tropical regions. Ideally, model parameterization of woody biomass thresholds should allow corresponding forest age being inferred, so that clearing of forest age class in the model could match that in the LUH1 data set. For this purpose, we fit a woody biomass-age curve for each forest PFT using the model data from the spin-up:

$$B = B_{max} \times [1 - \exp(-k \times age)] \qquad \text{Eq (2)}$$

where B_{max} is the asymptotic maximum woody biomass; k represents the biomass turnover rate. The curve-fitting used PFT-specific woody biomass time series during spin-up by averaging all grid cells across the globe. The ratios of thresholds of each age class to the maximum biomass (B_{max}) are looked up from this curve, based on their corresponding forest age (Table 2). Next, these ratios are multiplied with the equilibrium woody biomass at each grid cell, to derive a spatial map of thresholds in woody biomass. We set the corresponding age for the 3rd oldest age class for tropical forests as 15 years, in line with the residence time of shifting cultivation assumed in LUH1. Considering that temperate and boreal forests grow slower than tropical ones, forest ages corresponding to the 3rd age classes are set as 20 and 30 years for temperate and boreal forests, respectively.

We used two age classes for each herbaceous PFT including natural grassland, cropland and pasture, representing high versus low soil carbon densities, respectively. The energy balance in ORCHIDEE-MICT-GLUC is resolved over the whole grid cell, and the hydrological balance is calculated over sub-grid soil tiles (bare soil, forest and herbs) rather than over each PFT. We thus expect the factors influencing soil carbon decomposition (i.e., soil temperature, soil moisture) to have little difference between different age classes of the same PFTs. This justifies the small number of age classes for herbaceous PFTs selected here as it can maximize computing efficiency.

In S_{age} simulations, clearing of forest in the process of land turnover starts from the 3rd oldest age class (Age3, corresponding to 15 year-old forest in tropics), and forest clearing for wood harvest starts from the 2nd oldest age class (Age2). Wood product pools resulting from net land use change and land turnover, and those from wood harvest are tracked separately in the model. However, land patches created from different LUC activities are not tracked individually, e.g., young forests re-established from land turnover and wood harvest are merged together. In this approach, it is not possible to attribute the carbon fluxes

into exact LUC processes, which explains why factorial simulations are needed to attribute contributions from different LUC processes. Within the model, wood harvest module is executed before the modules of net land use change and land turnover. This is reasonable as a forest might be harvested prior to being converted to agricultural land. Last, we turned off the dynamic vegetation module as allowing dynamic vegetation and backcasting historical land cover maps using prescribed land transitions are internally inconsistent.

3 Results

3.1 Global carbon emissions with and without sub-grid age dynamics

Simulated E_{LUC} for 1501-2005 for different LUC processes and model configurations are shown in Fig. 1. The model simulates a cumulative $E_{LUC\ net}$ of 123.7 and 118.0 Pg C for 1501-2005, for cases of without and with sub-grid age dynamics, respectively. Including land turnover and wood harvest yields additional carbon emissions in both cases, with $E_{LUC\ turnover}$ as 45.4 Pg C and $E_{LUC\ harvest}$ as 27.4 Pg C in $S_{ageless}$. Accounting for age dynamics, in contrast, generates a lower $E_{LUC\ turnover}$ of 27.3 Pg C, or 40% lower than that obtained by the $S_{ageless}$ simulation. $E_{LUC\ harvest}$ for S_{age} equals to 30.8 Pg C and is slightly higher than in $S_{ageless}$.

We also compared the simulated global carbon balance with the annual updates by Le Quéré et al. (2016). Simulated $E_{LUC\ all}$ for 1959-2005 are 73.1 and 64.3 Pg C for $S_{ageless}$ and S_{age} simulations, respectively, with the carbon sinks when not accounting for land use change (i.e., NBP simulated by S0 simulations) as 118.0 and 119.2 Pg C. For comparison, Le Quéré et al. (2016) reported the cumulative carbon emissions from land use change for 1959-2005 as 66.4 Pg C and a residual carbon sink (i.e., residual term between anthropogenic fossil and land use emissions and the sum of atmospheric carbon growth and ocean carbon stock increase, equivalent to the land sink without any LUC) of 89.2 Pg C. Our estimated E_{LUC} are close to Le Quéré et al. (2016), however simulated carbon sinks without any LUC are much higher.

Figure 2 shows the time series of simulated $E_{LUC,\ all}$ from all LUC processes (net land use change + land turnover + wood harvest) in comparison with previous studies. Simulated E_{LUC} from each individual LUC process and corresponding time series of LUC areas are shown in Fig. 3. All estimations show a gradual increase of E_{LUC} starting from the early 18th century with a peak of 1.5–3.5 Pg C yr^{-1} around the 1950s, followed by a slight decrease during 1970s and 1980s and then another peak appeared for 1990s. E_{LUC} simulated by ORCHIDEE-MICT-GLUC is at the lower bound of all estimations until 1950s, but its second peak of emissions around 1990s (1.7–1.8 PgC yr^{-1}) is a little higher than the first one (1.5 Pg C yr^{-1}). $E_{LUC\ all,\ ageless}$ remains slightly higher than $E_{LUC\ all,\ age}$ until ca. 1960, and after that the difference

Biogeosciences Discuss., https://doi.org/10.5194/bg-2017-329
Manuscript under review for journal Biogeosciences
Discussion started: 4 September 2017

341 increases to 0.25 Pg C yr^{-1}. This two-peak pattern over time in $E_{LUC\ all}$ by ORCHIDEE-MICT-GLUC is
342 mainly driven by $E_{LUC\ net}$ (Fig. 3a) which also shows two peaks around 1950s and 1990s, consistent with
343 the peaks of land use change areas in the LUH1 forcing data (Fig. 3d). It should also be noted that as E_{LUC}
344 is quantified as the difference in NBP between two model simulations, its magnitude thus depend both on
345 the magnitude of areas subject to LUC and the magnitude of carbon fluxes in the reference S0
346 simulations, as driven by climate variability, atmospheric CO_2, etc.
347
348 Consistent with the idealized site-scale simulation in Yue et al. (2017), $E_{LUC\ turnover,\ ageless}$ is higher than
349 $E_{LUC\ turnvoer,\ age}$ (Fig. 3b). Emissions from instantaneous fluxes and harvested wood product pool are lower
350 in the S_{age} simulation than in S_{age} because in the former case low-biomass secondary forests are converted
351 to agricultural land, as opposed to high-biomass mature forests in the latter one. The difference in E_{LUC}
352 $_{turnover}$ between the two simulations explains the higher $E_{LUC\ all}$ obtained by the $S_{ageless}$ simulation. On the
353 other hand, $E_{LUC\ net}$ does not differ much between the two simulations (Fig. 3a), since in both cases it is
354 mature forests that are converted, which have little difference in their biomass densities between $S_{ageless}$
355 and S_{age}. Both $E_{LUC\ turnover,\ ageless}$ and $E_{LUC\ turnover,\ age}$ roughly follow the temporal pattern of areas impacted
356 by land turnover from LUH1 (Fig. 3e), with a steep increase starting from ca. 1900 until 1980,
357 corresponding to a strong increase in the areas undergoing forest-pasture gross transitions, dominated by
358 tropical regions. After 1980 the turnover-impacted area somewhat stabilizes and then shows a slight
359 decrease. Accordingly, $E_{LUC\ turnover,\ ageless}$ shows only a corresponding slight decrease of emissions in Fig.
360 3b, while $E_{LUC\ turnover,\ age}$ has a much bigger decrease, driven by the fact that recovering secondary forests
361 gain carbon quickly after being taken out of shifting agriculture systems.
362
363 Finally, $E_{LUC\ harvest}$ between S_{age} and $S_{ageless}$ simulations are almost identical until 1800 (Fig. 3), during
364 which the wood harvest area remains stable (Fig. 3f). After this, $E_{LUC\ harvest,\ ageless}$ is lower than $E_{LUC\ harvest,}$
365 $_{age}$ for the 19th and most of the 20th century when $E_{LUC\ harvest}$ continued to rise, mainly driven by a rise in
366 secondary forest harvest area (Fig. 3f). According to the priority rules of secondary forest harvest in S_{age},
367 older forests, until the oldest ones, will be harvested if existing young forest age classes are not sufficient
368 to meet the prescribed harvest target. This most likely happens when harvested area continues to rise,
369 simply because existing secondary forests as a legacy of historical land use change cannot meet the
370 increasing demand. This exemplifies the potential inconsistencies between model structure and forcing
371 data. In addition, under such a circumstance, old forests in S_{age} simulation tend to have higher biomass
372 density than the ageless forests in $S_{ageless}$, because in the former case these mature forests remain intact
373 throughout the whole simulation, while in the latter case the ageless forests in $S_{ageless}$ have been

374 "degraded" due to historical LUC activities. This explains the slightly higher $E_{LUC\ harvest}$ in the S_{age}
375 simulation.
376
377 **3.2 Spatial distribution of land use change emissions**
378 Figure 4 shows the spatial distribution of cumulative E_{LUC} for 1501–2005 from different LUC processes
379 in the $S_{ageless}$ simulations (Fig. 4a–c), the difference in E_{LUC} between S_{age} and $S_{ageless}$ simulations (Fig. 4d–
380 f), corresponding net forest area change (Fig. 4g) and areas subject to land turnover (Fig. 4h) and wood
381 harvest (Fig. 4i). The spatial pattern of $E_{LUC\ net}$ generally resembles that of forest area loss, with large
382 areas of forests being cleared and corresponding high $E_{LUC\ net}$ in eastern North America, South America
383 and Africa, southern and eastern Asia, and in central Eurasia (Fig. 4a, Fig. 4g). Central and Eastern
384 Europe show some increases in forest area but carbon emissions from net land use change persists,
385 probably because forest recovery happened in recent times and carbon accumulation in recovering forests
386 is not yet big enough to compensate for historical loss (e.g., see Fig. 6f). Depending on different regions,
387 $E_{LUC\ net,\ age}$ is slightly higher (e.g., along the boreal forest belt in central Europe and Asia, woodland
388 savanna in South America) or lower (e.g., part of Africa and Australia) than $E_{LUC\ net,\ ageless}$ (Fig. 4d). This
389 difference between S_{age} and $S_{ageless}$ is in general of rather low magnitude (<0.5 kg C m^{-2} over 1501-2005).
390 It mainly depends on the age classes of forests to be cleared in the S_{age} simulation and how the forest
391 biomass density compares with that from $S_{ageless}$ simulation and whether biomass density of the single
392 ageless mature patch is diluted or not with establishment of young forests.
393
394 In the LUH1 data set, shifting cultivation (land turnover here) is limited to the tropical region (Fig. 4h), as
395 in the original LUH1 forcing data. Tropical Africa is the region with most of the turnover activities, and
396 consequently has highest $E_{LUC\ turnover}$. Note the peripheral of Amazon basin also show active shifting
397 cultivations and resulting carbon emissions (Fig. 4b, Fig. 4h). $E_{LUC\ turnover,\ age}$ is in general lower than E_{LUC}
398 $_{tunrnover,\ ageless}$ everywhere except at the northern fringe of northern African woodland savanna (Fig. 4e).
399 Last, wood harvest mainly occurs in temperate and boreal forest in Northern Hemisphere (Europe and
400 central Siberia, eastern North America and southern and eastern Asia) and tropical forests including those
401 of Amazon forest, in central Africa and tropical Asia, with corresponding carbon emissions (Fig. 4c, Fig.
402 4i). $E_{LUC\ harvest,\ age}$ is a higher source than $E_{LUC\ harvest,\ ageless}$ for most of the harvested regions, which mainly
403 results from the model feature as explained above.
404
405 **3.3 Simulated regional LUC emissions**
406 Estimated carbon emissions since 1900 from different regions are shown in Fig. 5, with emissions from
407 each LUC source for $S_{ageless}$ simulation being shown in Fig. S7. The corresponding areas subject to the

three LUC processes with forests being mainly involved are shown in Fig. 6. We also compared our estimations by Stocker et al. (2014), where the LUC emissions are simulated with a different vegetation model (LPX-Bern) but contributions of each individual LUC process is quantified with a similar approach as ours. Both studies are forced by the LUH1 data set, although actual areas undergoing different land use change activities may slightly differ because of different LUC implementation strategies. As shown in Fig. 6, in spite of incessant episodic forest gains, for most time in most regions, historical net forest change was dominated by forest loss, except for the latter half of the 20th century in Western Europe, Former Soviet Union (FSU), and for the time period after 1970 in Pacific Developed Region. Meanwhile, land turnover and wood harvest persisted for most regions, although their magnitudes varied over time. While forest gain can lead to carbon uptake, it could be outweighed by emissions from simultaneous forest loss (note here both forest loss and gain occurred as a result of net land use change within the same region but not within the same grid cell), land turnover and wood harvest. Thus it is not surprising that for most regions and most time, LUC impacts on carbon cycle are diagnosed as emissions, except for the latter half the 20th century for Former Soviet Union (Fig. 5).

The two estimations of LUC emissions from our study and Stocker et al. (2014) are in general agreement for most of the regions, including their temporal variations. Emissions globally are dominated by Central and South America and Africa & Middle East. Emissions increased in both regions since 1900, and a peak of emissions occurred around the middle of the 20th century in Africa and around 1980 in Central and South America (Fig. 5a, 5c). Emissions in Stocker et al. (2014) show similar temporal variations for these two regions as in our study. The peak of emissions in Africa & Middle East around 1950 is clearly dominated by a peak of forest loss due to net land use change (red line in Fig. 6c), and a surge of forest loss due to land turnover that has accelerated between 1940 and 1960 (green line in Fig. 6c). After that emissions decreased slightly, mainly due to the stabilized land turnover activities and a drop in area of net land use change. Then the emissions slightly increased again around 1980s, due to an increase in forest loss of net land use change (red line in Fig. 6c) and wood harvest (cyan line in Fig. 6c). In contrast, even with a similar peak of forest loss due to net land use change in Central and South America as in Africa & Middle East, as shown in Fig. 6a (red line), emissions in the former region continued to increase until 1980s (Fig. 5a), mainly due to continuous growing of forest losses resulting from land turnover (green line in Fig. 6a).

Both South & Southeast Asia and China Region showed steady increase in emissions up to c.a. 1990s (Fig. 5b, 5e). In the former case, this is likely driven by continuous growing land turnover and wood harvest; in the latter case, it is more likely driven by growing net forest loss (Fig. 6b, 6e). The peak in

emissions around 1990s in China Region echoes a peak in net forest loss (red line in Fig. 6e). Stocker et al. (2014) shows slightly higher emissions than our estimates for South & Southeast Asia, and lower magnitude in China Region, but with similar temporal patterns in both regions. For the three regions where land turnover activities are included in the LUH1 data set (i.e., Central and South America, South & Southeast Asia, and Africa & Middle East), there are some periods during which $E_{LUC\ ageless}$ is clearly higher than $E_{LUC\ age}$. These mainly correspond to the time when land turnover area either showed decelerated growth or stabilized, being roughly after 1970 in Central and South America (Fig. 5a), after 1980 in South & Southeast Asia (Fig. 5b), and 1965-1985 in Africa & Middle East (Fig. 5c).

North America shows most clearly the legacy impact of past LUC activities on LUC emissions. For the period 1900–1940, carbon emissions in North America gradually decreased even though areas subject to forest loss and wood harvest showed slight increases (Fig. 5d, Fig. 6d). This is likely due to the year 1900 is preceded by a peak of net forest loss, which yielded a high emission legacy for the several beginning decades in the 20th century. LUC emissions and sinks in Europe and Pacific Developed Region are of very small magnitudes, despite a high forest wood harvest area in Europe. This is because in general $E_{LUC\ harvest}$ is small compared to $E_{LUC\ net}$, probably due to the biomass accumulation in re-growing forest (Fig. S7). The carbon sink brought about by net forest gain is the most prominent in Former Soviet Union (blue line in Fig. 6g), where a peak of forest gain around 1950s lead to a sustained sink of ~0.1 PgC yr^{-1} for the latter half of the 20th century (Fig. 5g), however, concurrent sink is not seen in Stocker et al. (2014).

4 Discussion

4.1 Impacts on estimated E_{LUC} by including gross land use change and sub-grid secondary forests

The significant advancement in this study in comparison with previous works, as far as we know, is the explicit inclusion of differently aged sub-grid secondary land cohorts in DGVMs. Although secondary lands have been represented in some DGVMs in previous studies (Shevliakova et al., 2009; Stocker et al., 2014; Yang et al., 2010), here we incorporated the concept of rotation cycle. This is particularly important in simulating the carbon cycle impacts of gross land use change, such as wood harvest and shifting cultivation. Because secondary lands, especially young re-growing forests, have lower biomass carbon stock than mature forests when they stay in rotation cycle of either shifting cultivation or forestry management (e.g., wood harvest). Consequently, related land use change emissions are lower than otherwise modeled without sub-grid age dynamics, which is equivalent to clearing of mature forests. Our results demonstrate that by explicitly including secondary forest cohorts, estimated carbon emissions from shifting cultivation for 1501–2005 are reduced from 45.4 Pg C to 27.4 Pg C, or 40% lower with age dynamics than without.

476

477 Table 3 summarized estimations of E_{LUC} from different studies by including both net transitions and gross
478 land use change, and the contributions to total emissions by including gross transitions. All studies show
479 that including gross land use change increased estimated carbon emissions. Stocker et al. (2014) reported
480 that gross change contributed 15% to total emissions, whereas Wilkenskjeld et al. (2014) reported a much
481 higher contribution of 38%. Hansis et al. (2015) by using a bookkeeping model, reported a 22–24%
482 contribution from gross change if cleared lands are primarily from primary lands, in contrast to a small
483 contribution of only 2% if cleared lands are exclusively from secondary lands. For the $S_{ageless}$ simulation
484 in the current study, the contribution from gross land use change to total emissions is 20%, falling in
485 between Stocker et al. (2014) and others including the 28% contribution by gross change in the tropics
486 reported by Houghton (2010). However, the simulation by including secondary land (i.e., S_{age}) gives a
487 lower gross land use change contribution (15%) than $S_{ageless}$. In general, the same model yields lower
488 contribution of gross changes by converting dominantly secondary land versus primary land (our study
489 and Hansis et al., 2015). Among different models/methods, the ones including secondary lands
490 (Houghton, 2010; Stocker et al., 2014) tends to yield lower contribution of gross changes than those do
491 not (Wilkenskjeld et al., 2014). Although the exact percentage might differ depending on the amount of
492 gross changes included, it seems that contributions from gross land use change are overestimated when
493 ignoring sub-grid secondary lands.
494
495 We also expected E_{LUC} from wood harvest to be smaller when including secondary forests, for the same
496 reason than shifting cultivation. However, we obtained a slightly higher $E_{LUC\ harvest,\ age}$ than $E_{LUC\ havrvest,\ agelss}$, mainly because there are not enough secondary forests available for harvesting in S_{age}, so that mature
498 forests with a higher biomass density than in $S_{ageless}$ are harvested according to the priority setting in the
499 model, which leads to higher emissions. This model feature was designed to address potential
500 inconsistencies between prescribed harvest area in the forcing data and (secondary) forest availability in
501 the model, to ensure that ultimately realized harvest area in the model is as close as possible to the
502 prescribed one. This is also due to the limitation that we implemented wood harvest based on input
503 information on harvested area rather than on wood volume. In the future, this process should be modified
504 so that harvested wood volume information is directly used in the model, to allow dynamic decision on
505 whether an old forest or secondary forest should be harvested.
506
507 **4.2 Impacts on estimated emissions by initial biomass stock**
508 As shown in Fig. 2 and Table 3, our estimations of historical LUC emissions from both $S_{ageless}$ and S_{age}
509 simulations are lower than other studies for most time of history (albeit close to Stocker et al. 2014 before

ca. 1860). We compared in Table S1 the cumulative E_{LUC} for 1850-2005 by our studies and several previous studies. Our estimates (147 Pg C for $E_{LUC\ age}$ and 158 Pg C for $E_{LUC\ ageless}$) are lower than the lower bound of other estimates (171 Pg C by Stocker et al. 2014). Estimations of Hansis et al. (2015) and Gasser and Ciais (2013) using Hurtt et al. (2006) data set give rather larger estimates than others, being 261 and 294 Pg C, respectively. The median value of all previous estimates cited in Table S1 yields 210 Pg C, still much higher than our estimates.

The lower estimates of E_{LUC} in our study are likely linked with underestimated global biomass carbon stock in ORCHIDEE-MICT-GLUC. The global biomass carbon stock simulated by our model at 1500 prior to any land use change is 365 Pg C, and increases to 510 Pg C at 2005 in the S0 simulations (i.e., assuming no LUC activity). The simulated global biomass remains almost unchanged in the S3 simulations where all three LUC processes are included. Avitabile et al. (2016) merged two tropical aboveground forest biomass data sets from Saatchi et al. (2011) and Baccini et al. (2012) with northern hemisphere volumetric forest stock growth data from Santoro et al. (2015). Their estimated global forest biomass for aboveground only is 505 Pg C. Our simulated contemporary global total biomass stock (i.e., from S3 simulations) is thus even lower than their estimate for aboveground biomass.

Li et al. (2017) has identified emergent linear relationship between cumulative E_{LUC} for 1901–2012 and initial biomass in 1901 among the nine DGVMs of the Trends in Net Land-Atmosphere Exchange (TRENDY-v2) project (http://dgvm.ceh.ac.uk/node/9) (shown in Fig. S8). They further used these relationships to obtain an observation-constrained E_{LUC} (horizontal orange line in Fig. S8) for 1901–2012 that are independent of DGVMs, by reconstructing an initial biomass carbon stock in 1901(vertical green line in Fig. S8) based on contemporary satellite observations of global biomass distribution. As is shown in Fig. S8, carbon stocks are indeed underestimated in our model for a few regions and the globe, compared to the satellite-based reconstructions of 1901 biomass in Li et al. (2017). We derive a biomass-corrected cumulative E_{LUC} for each region and the globe for 1901-2005, by using the relationships between cumulative E_{LUC} and initial 1901 biomass among different DGVMs, as shown in Fig. S8. The biomass-corrected cumulative E_{LUC} for 1501–2005 and 1850–2005 are further derived, by assuming the same ratio between biomass-corrected and original cumulative E_{LUC} for these two periods against that of 1901–2005. The original and biomass-corrected cumulative E_{LUC} for 1501–2005, 1850–2005 and 1901–2005 and the correction ratios for each region and the globe are summarized in Table S2.

The biomass-corrected global cumulative E_{LUC} for 1850–2005 are 174–207 Pg C for the $S_{ageless}$ simulation, and 161–194 Pg C for the S_{age} simulation (Table S1). These are in closer agreement with the

544 median value of previous studies (210 Pg C). In addition, the magnitude of historical LUC activities
545 actually included in our simulation is lower than that prescribed in the original LUH1 data set, as an
546 inevitable result from the reconciliation between LUH1 data set and the used ESA CCI 2005 PFT map
547 (Fig. S2). Almost 30% of transitions from natural land to pasture, and 15% of transitions from natural
548 land to croplands as a result of net land use change were omitted when implementing the LUH1 data set
549 in our model. About 15% of the transitions between secondary land and pasture as land turnover were
550 omitted as well. If these omitted transitions were taken into account, estimated cumulative E_{LUC} would
551 have been even larger.
552
553 **4.3 Land use and management processes in DGVMs in relation to forest demography**
554 Forest demography is an important factor in determining forest carbon dynamics at both stand and
555 regional scales (Amiro et al., 2010; Pan et al., 2011). Natural disturbances (such as fire, wind and insect)
556 and land use change including land management are two primary factors creating spatial heterogeneity in
557 forest age. As more and more forests are now under human management with differed intensities (Erb et
558 al., 2017; Luyssaert et al., 2014), sub-grid forest demography should be incorporated in DGVMs to
559 account for the management consequences. Furthermore, when making more accurate (and detailed)
560 account of regional carbon balances linked with land use change, other land cover types than forests
561 should be distinguished into different cohorts as well, because the presence of many nonlinear processes
562 (e.g., soil carbon decomposition) makes the simple averaging scheme as in the case where they're
563 represented with a single patch within the model a sub-optimal choice. This new model structure, to have
564 more than one cohort for the same land cover within a grid cell, as is partly explored by Shevliakova et al.
565 (2009) as well in a dynamic land model LM3V less complex than ORCHIDEE-MICT-GLUC, will have
566 impact on simulated biogeochemical and biophysical processes, as partly demonstrated here.
567
568 However, despite these improvements in model structure, it remains a big challenge to "seamlessly"
569 integrate land use change forcing data into the model. The fundamental reason is that historical transitions
570 of land use change are not reconstructed in a way being internally consistent with DGVMs. The system to
571 build historical LUC transitions (so-called LUC model) and DGVMs may use different land cover types
572 so that conciliating the two land cover maps is inevitable. This will lead to loss of information in
573 incorporating forcing data into the model, as is pointed out also by Stocker et al. (2014). Second,
574 simulated forest biomass density might be different as well, so that the same amount of harvested wood
575 volume will translate into different forest areas in the LUC model and DGVMs. Recently progresses have
576 been made in DGVMs to represent forest stand structure and detailed management options (Naudts et al.,
577 2015), so that wood volume information can be used directly as a forcing in the model to drive forestry

decisions. Third, LUC model uses assumptions on rotation lengths of shifting cultivation or forest management, and information generated there might not be consistent with forest age distribution in DGVMs, as is the case in our study.

To remove these obstacles and allow a more comprehensive integration of land use change information into DGVMs, one possible route is to further develop DGVMs to partly embed functions of LUC models. This will allow DGVMs to be used in an "inversed" manner than its current way of utilization. For example, food demand could be used as an input, so that dynamical decisions could be made within the model on how many croplands need to be created given the simulated crop yield by the crop module inside the DGVM. The same case also applies on pasture. Grassland management modules within DGVMs could generate information on meat and milk production etc., and this information could be used to inverse the meat and mild demand into demanded pasture areas (Chang et al., 2016). Harvested wood for a certain product usage might need wood with a specific diameter range, corresponding to a certain forest age class given their simulated growth state, allowing the determination of both ages and areas of forests to be harvested.

5 Conclusions

In this study, we investigated the impacts on estimated historical gross land use change emissions by accounting for sub-grid secondary land cohorts in a dynamic global vegetation model. The model employed here is capable of representing the rotation processes in land use and land management that mainly involve secondary forests, such as shifting cultivation and forest wood harvest. Intermediately-aged secondary forests are given a high priority when forest clearing occurs in either shifting cultivation or wood harvest, complemented by older forests if young ones are insufficient to meet the prescribed land use transition. For the land use transition that entails a net change in the land cover, clearing of forests start exclusively from mature forests and move sequentially to younger forests when older ones are used up. This set of rules becomes indispensible when incorporating sub-grid secondary land cohorts and external land use transition forcing data in the model. As such, the simulated portfolio of secondary land cohorts within the model is driven by a reconstruction of historical gross land use change.

We found that over 1501-2005, accounting for sub-grid secondary land cohorts yields lower land use change emissions than not, which is dominated by lower emissions from shifting cultivation. This is because secondary forests with a lower biomass are allowed being cleared, instead of the mature forests with a high biomass as in the traditional approach to representing forest with a single sub-tile in the model. Obviously, our conclusion and the extent to which emissions from shifting cultivation can be down-

estimated are closely linked with the priority rules regarding which land cohorts to target in land use change, as described above. Nevertheless, we point out that emissions from gross land use change, which were formerly ignored in modeling studies focusing on net transitions only, might have been overestimated if the sub-grid secondary forests are not accounted for. This will lead to a lower-than-assumed so-called residual land CO_2 sink on undisturbed land, which is inferred from the net balance of emissions from fossil fuel and land use change, and CO_2 sinks in the atmosphere and ocean.

References:

Amiro, B. D., Barr, A. G., Barr, J. G., Black, T. A., Bracho, R., Brown, M., Chen, J., Clark, K. L., Davis, K. J., Desai, A. R., Dore, S., Engel, V., Fuentes, J. D., Goldstein, A. H., Goulden, M. L., Kolb, T. E., Lavigne, M. B., Law, B. E., Margolis, H. A., Martin, T., McCaughey, J. H., Misson, L., Montes-Helu, M., Noormets, A., Randerson, J. T., Starr, G. and Xiao, J.: Ecosystem carbon dioxide fluxes after disturbance in forests of North America, J. Geophys. Res., 115(G4), G00K02, doi:10.1029/2010JG001390, 2010.

Avitabile, V., Herold, M., Heuvelink, G. B. M., Lewis, S. L., Phillips, O. L., Asner, G. P., Armston, J., Ashton, P. S., Banin, L., Bayol, N., Berry, N. J., Boeckx, P., de Jong, B. H. J., DeVries, B., Girardin, C. A. J., Kearsley, E., Lindsell, J. A., Lopez-Gonzalez, G., Lucas, R., Malhi, Y., Morel, A., Mitchard, E. T. A., Nagy, L., Qie, L., Quinones, M. J., Ryan, C. M., Ferry, S. J. W., Sunderland, T., Laurin, G. V., Gatti, R. C., Valentini, R., Verbeeck, H., Wijaya, A. and Willcock, S.: An integrated pan-tropical biomass map using multiple reference datasets, Glob Change Biol, 22(4), 1406–1420, doi:10.1111/gcb.13139, 2016.

Baccini, A., Goetz, S. J., Walker, W. S., Laporte, N. T., Sun, M., Sulla-Menashe, D., Hackler, J., Beck, P. S. A., Dubayah, R., Friedl, M. A., Samanta, S. and Houghton, R. A.: Estimated carbon dioxide emissions from tropical deforestation improved by carbon-density maps, Nature Clim. Change, 2(3), 182–185, doi:10.1038/nclimate1354, 2012.

Chang, J., Ciais, P., Herrero, M., Havlik, P., Campioli, M., Zhang, X., Bai, Y., Viovy, N., Joiner, J., Wang, X., Peng, S., Yue, C., Piao, S., Wang, T., Hauglustaine, D. A., Soussana, J.-F., Peregon, A., Kosykh, N. and Mironycheva-Tokareva, N.: Combining livestock production information in a process-based vegetation model to reconstruct the history of grassland management, Biogeosciences, 13(12), 3757–3776, doi:10.5194/bg-13-3757-2016, 2016.

Chazdon, R. L., Broadbent, E. N., Rozendaal, D. M. A., Bongers, F., Zambrano, A. M. A., Aide, T. M., Balvanera, P., Becknell, J. M., Boukili, V., Brancalion, P. H. S., Craven, D., Almeida-Cortez, J. S., Cabral, G. A. L., Jong, B. de, Denslow, J. S., Dent, D. H., DeWalt, S. J., Dupuy, J. M., Durán, S. M., Espírito-Santo, M. M., Fandino, M. C., César, R. G., Hall, J. S., Hernández-Stefanoni, J. L., Jakovac, C. C., Junqueira, A. B., Kennard, D., Letcher, S. G., Lohbeck, M., Martínez-Ramos, M., Massoca, P., Meave, J. A., Mesquita, R., Mora, F., Muñoz, R., Muscarella, R., Nunes, Y. R. F., Ochoa-Gaona, S., Orihuela-Belmonte, E., Peña-Claros, M., Pérez-García, E. A., Piotto, D., Powers, J. S., Rodríguez-Velazquez, J., Romero-Pérez, I. E., Ruíz, J., Saldarriaga, J. G., Sanchez-Azofeifa, A., Schwartz, N. B., Steininger, M. K., Swenson, N. G., Uriarte, M., Breugel, M. van, Wal, H. van der, Veloso, M. D. M., Vester, H., Vieira, I. C. G., Bentos, T. V., Williamson, G. B. and Poorter, L.: Carbon sequestration potential of second-growth forest regeneration in the Latin American tropics, Science Advances, 2(5), e1501639, doi:10.1126/sciadv.1501639, 2016.

654 Don, A., Schumacher, J. and Freibauer, A.: Impact of tropical land-use change on soil organic carbon
655 stocks – a meta-analysis, Global Change Biology, 17(4), 1658–1670, doi:10.1111/j.1365-
656 2486.2010.02336.x, 2011.

657 Erb, K.-H., Luyssaert, S., Meyfroidt, P., Pongratz, J., Don, A., Kloster, S., Kuemmerle, T., Fetzel, T.,
658 Fuchs, R., Herold, M., Haberl, H., Jones, C. D., Marín-Spiotta, E., McCallum, I., Robertson, E., Seufert,
659 V., Fritz, S., Valade, A., Wiltshire, A. and Dolman, A. J.: Land management: data availability and process
660 understanding for global change studies, Glob Change Biol, 23(2), 512–533, doi:10.1111/gcb.13443,
661 2017.

662 Gasser, T. and Ciais, P.: A theoretical framework for the net land-to-atmosphere CO2 flux and its
663 implications in the definition of "emissions from land-use change," Earth Syst. Dynam., 4(1), 171–186,
664 doi:10.5194/esd-4-171-2013, 2013.

665 Guimberteau, M., Zhu, D., Maignan, F., Huang, Y., Yue, C., Dantec-Nédélec, S., Ottlé, C., Jornet-Puig,
666 A., Bastos, A., Laurent, P., Goll, D., Bowring, S., Chang, J., Guenet, B., Tifafi, M., Peng, S., Krinner, G.,
667 Ducharne, A., Wang, F., Wang, T., Wang, X., Wang, Y., Yin, Z., Lauerwald, R., Joetzjer, E., Qiu, C.,
668 Kim, H. and Ciais, P.: ORCHIDEE-MICT (revision 4126), a land surface model for the high-latitudes:
669 model description and validation, Geosci. Model Dev. Discuss., 2017, 1–65, doi:10.5194/gmd-2017-122,
670 2017.

671 Hansis, E., Davis, S. J. and Pongratz, J.: Relevance of methodological choices for accounting of land use
672 change carbon fluxes, Global Biogeochem. Cycles, 29(8), 2014GB004997, doi:10.1002/2014GB004997,
673 2015.

674 Houghton, R. A.: The annual net flux of carbon to the atmosphere from changes in land use 1850–1990*,
675 Tellus B, 51(2), 298–313, doi:10.1034/j.1600-0889.1999.00013.x, 1999.

676 Houghton, R. A.: Revised estimates of the annual net flux of carbon to the atmosphere from changes in
677 land use and land management 1850–2000, Tellus B, 55(2), 378–390, doi:10.1034/j.1600-
678 0889.2003.01450.x, 2003.

679 Houghton, R. A.: How well do we know the flux of CO2 from land-use change?, Tellus B, 62(5), 337–
680 351, doi:10.1111/j.1600-0889.2010.00473.x, 2010.

681 Houghton, R. A., House, J. I., Pongratz, J., van der Werf, G. R., DeFries, R. S., Hansen, M. C., Le Quéré,
682 C. and Ramankutty, N.: Carbon emissions from land use and land-cover change, Biogeosciences, 9(12),
683 5125–5142, doi:10.5194/bg-9-5125-2012, 2012.

684 Hurtt, G. C., Frolking, S., Fearon, M. G., Moore, B., Shevliakova, E., Malyshev, S., Pacala, S. W. and
685 Houghton, R. A.: The underpinnings of land-use history: three centuries of global gridded land-use
686 transitions, wood-harvest activity, and resulting secondary lands, Global Change Biology, 12(7), 1208–
687 1229, doi:10.1111/j.1365-2486.2006.01150.x, 2006.

688 Hurtt, G. C., Chini, L. P., Frolking, S., Betts, R. A., Feddema, J., Fischer, G., Fisk, J. P., Hibbard, K.,
689 Houghton, R. A., Janetos, A., Jones, C. D., Kindermann, G., Kinoshita, T., Goldewijk, K. K., Riahi, K.,
690 Shevliakova, E., Smith, S., Stehfest, E., Thomson, A., Thornton, P., Vuuren, D. P. van and Wang, Y. P.:
691 Harmonization of land-use scenarios for the period 1500–2100: 600 years of global gridded annual land-
692 use transitions, wood harvest, and resulting secondary lands, Climatic Change, 109(1–2), 117,
693 doi:10.1007/s10584-011-0153-2, 2011.

694 Jain, A. K., Meiyappan, P., Song, Y. and House, J. I.: CO2 emissions from land-use change affected more
695 by nitrogen cycle, than by the choice of land-cover data, Glob Change Biol, 19(9), 2893–2906,
696 doi:10.1111/gcb.12207, 2013.

697 Krinner, G., Viovy, N., de Noblet-Ducoudré, N., Ogée, J., Polcher, J., Friedlingstein, P., Ciais, P., Sitch,
698 S. and Prentice, I. C.: A dynamic global vegetation model for studies of the coupled atmosphere-
699 biosphere system, Global Biogeochemical Cycles, 19(1), GB1015, doi:10.1029/2003GB002199, 2005.

700 Le Quéré, C., Andrew, R. M., Canadell, J. G., Sitch, S., Korsbakken, J. I., Peters, G. P., Manning, A. C.,
701 Boden, T. A., Tans, P. P., Houghton, R. A., Keeling, R. F., Alin, S., Andrews, O. D., Anthoni, P.,
702 Barbero, L., Bopp, L., Chevallier, F., Chini, L. P., Ciais, P., Currie, K., Delire, C., Doney, S. C.,
703 Friedlingstein, P., Gkritzalis, T., Harris, I., Hauck, J., Haverd, V., Hoppema, M., Klein Goldewijk, K.,
704 Jain, A. K., Kato, E., Körtzinger, A., Landschützer, P., Lefèvre, N., Lenton, A., Lienert, S., Lombardozzi,
705 D., Melton, J. R., Metzl, N., Millero, F., Monteiro, P. M. S., Munro, D. R., Nabel, J. E. M. S., Nakaoka,
706 S., O'Brien, K., Olsen, A., Omar, A. M., Ono, T., Pierrot, D., Poulter, B., Rödenbeck, C., Salisbury, J.,
707 Schuster, U., Schwinger, J., Séférian, R., Skjelvan, I., Stocker, B. D., Sutton, A. J., Takahashi, T., Tian,
708 H., Tilbrook, B., Laan-Luijkx, I. T. van der, Werf, G. R. van der, Viovy, N., Walker, A. P., Wiltshire, A.
709 J. and Zaehle, S.: Global Carbon Budget 2016, Earth System Science Data, 8(2), 605–649,
710 doi:10.5194/essd-8-605-2016, 2016.

711 Li, W., Ciais, P., Peng, S., Yue, C., Wang, Y., Thurner, M., Saatchi, S. S., Arneth, A., Avitabile, V.,
712 Carvalhais, N., Harper, A. B., Kato, E., Koven, C., Liu, Y. Y., Nabel, J. E. M. S., Pan, Y., Pongratz, J.,
713 Poulter, B., Pugh, T. A. M., Santoro, M., Sitch, S., Stocker, B. D., Viovy, N., Wiltshire, A., Yousefpour,
714 R. and Zaehle, S.: Land-use and land-cover change carbon emissions between 1901 and 2012 constrained
715 by biomass observations, Biogeosciences Discuss., 2017, 1–25, doi:10.5194/bg-2017-186, 2017.

716 Luyssaert, S., Jammet, M., Stoy, P. C., Estel, S., Pongratz, J., Ceschia, E., Churkina, G., Don, A., Erb, K.,
717 Ferlicoq, M., Gielen, B., Grünwald, T., Houghton, R. A., Klumpp, K., Knohl, A., Kolb, T., Kuemmerle,
718 T., Laurila, T., Lohila, A., Loustau, D., McGrath, M. J., Meyfroidt, P., Moors, E. J., Naudts, K., Novick,
719 K., Otto, J., Pilegaard, K., Pio, C. A., Rambal, S., Rebmann, C., Ryder, J., Suyker, A. E., Varlagin, A.,
720 Wattenbach, M. and Dolman, A. J.: Land management and land-cover change have impacts of similar
721 magnitude on surface temperature, Nature Clim. Change, 4(5), 389–393, doi:10.1038/nclimate2196,
722 2014.

723 Naudts, K., Ryder, J., McGrath, M. J., Otto, J., Chen, Y., Valade, A., Bellasen, V., Berhongaray, G.,
724 Bönisch, G., Campioli, M., Ghattas, J., De Groote, T., Haverd, V., Kattge, J., MacBean, N., Maignan, F.,
725 Merilä, P., Penuelas, J., Peylin, P., Pinty, B., Pretzsch, H., Schulze, E. D., Solyga, D., Vuichard, N., Yan,
726 Y. and Luyssaert, S.: A vertically discretised canopy description for ORCHIDEE (SVN r2290) and the
727 modifications to the energy, water and carbon fluxes, Geosci. Model Dev., 8(7), 2035–2065,
728 doi:10.5194/gmd-8-2035-2015, 2015.

729 Pan, Y., Chen, J. M., Birdsey, R., McCullough, K., He, L. and Deng, F.: Age structure and disturbance
730 legacy of North American forests, Biogeosciences, 8(3), 715–732, doi:10.5194/bg-8-715-2011, 2011.

731 Peng, S., Ciais, P., Maignan, F., Li, W., Chang, J., Wang, T. and Yue, C.: Sensitivity of land use change
732 emission estimates to historical land use and land cover mapping, Global Biogeochem. Cycles, 31(4),
733 2015GB005360, doi:10.1002/2015GB005360, 2017.

734 Piao, S., Fang, J., Ciais, P., Peylin, P., Huang, Y., Sitch, S. and Wang, T.: The carbon balance of
735 terrestrial ecosystems in China, Nature, 458(7241), 1009–1013, doi:10.1038/nature07944, 2009.

Poeplau, C., Don, A., Vesterdal, L., Leifeld, J., Van Wesemael, B., Schumacher, J. and Gensior, A.: Temporal dynamics of soil organic carbon after land-use change in the temperate zone – carbon response functions as a model approach, Global Change Biology, 17(7), 2415–2427, doi:10.1111/j.1365-2486.2011.02408.x, 2011.

Pongratz, J., Reick, C. H., Raddatz, T. and Claussen, M.: Effects of anthropogenic land cover change on the carbon cycle of the last millennium, Global Biogeochem. Cycles, 23(4), GB4001, doi:10.1029/2009GB003488, 2009.

Pongratz, J., Reick, C. H., Houghton, R. A. and House, J. I.: Terminology as a key uncertainty in net land use and land cover change carbon flux estimates, Earth Syst. Dynam., 5(1), 177–195, doi:10.5194/esd-5-177-2014, 2014.

Poorter, L., Bongers, F., Aide, T. M., Almeyda Zambrano, A. M., Balvanera, P., Becknell, J. M., Boukili, V., Brancalion, P. H. S., Broadbent, E. N., Chazdon, R. L., Craven, D., de Almeida-Cortez, J. S., Cabral, G. A. L., de Jong, B. H. J., Denslow, J. S., Dent, D. H., DeWalt, S. J., Dupuy, J. M., Durán, S. M., Espírito-Santo, M. M., Fandino, M. C., César, R. G., Hall, J. S., Hernandez-Stefanoni, J. L., Jakovac, C. C., Junqueira, A. B., Kennard, D., Letcher, S. G., Licona, J.-C., Lohbeck, M., Marín-Spiotta, E., Martínez-Ramos, M., Massoca, P., Meave, J. A., Mesquita, R., Mora, F., Muñoz, R., Muscarella, R., Nunes, Y. R. F., Ochoa-Gaona, S., de Oliveira, A. A., Orihuela-Belmonte, E., Peña-Claros, M., Pérez-García, E. A., Piotto, D., Powers, J. S., Rodríguez-Velázquez, J., Romero-Pérez, I. E., Ruíz, J., Saldarriaga, J. G., Sanchez-Azofeifa, A., Schwartz, N. B., Steininger, M. K., Swenson, N. G., Toledo, M., Uriarte, M., van Breugel, M., van der Wal, H., Veloso, M. D. M., Vester, H. F. M., Vicentini, A., Vieira, I. C. G., Bentos, T. V., Williamson, G. B. and Rozendaal, D. M. A.: Biomass resilience of Neotropical secondary forests, Nature, 530(7589), 211–214, doi:10.1038/nature16512, 2016.

Prestele, R., Arneth, A., Bondeau, A., de Noblet-Ducoudré, N., Pugh, T. A. M., Sitch, S., Stehfest, E. and Verburg, P. H.: Current challenges of implementing land-use and land-cover change in climate assessments, Earth Syst. Dynam. Discuss., 2016, 1–28, doi:10.5194/esd-2016-39, 2016.

Saatchi, S. S., Harris, N. L., Brown, S., Lefsky, M., Mitchard, E. T. A., Salas, W., Zutta, B. R., Buermann, W., Lewis, S. L., Hagen, S., Petrova, S., White, L., Silman, M. and Morel, A.: Benchmark map of forest carbon stocks in tropical regions across three continents, PNAS, doi:10.1073/pnas.1019576108, 2011.

Santoro, M., Beaudoin, A., Beer, C., Cartus, O., Fransson, J. E. S., Hall, R. J., Pathe, C., Schmullius, C., Schepaschenko, D., Shvidenko, A., Thurner, M. and Wegmüller, U.: Forest growing stock volume of the northern hemisphere: Spatially explicit estimates for 2010 derived from Envisat ASAR, Remote Sensing of Environment, 168, 316–334, doi:10.1016/j.rse.2015.07.005, 2015.

Shevliakova, E., Pacala, S. W., Malyshev, S., Hurtt, G. C., Milly, P. C. D., Caspersen, J. P., Sentman, L. T., Fisk, J. P., Wirth, C. and Crevoisier, C.: Carbon cycling under 300 years of land use change: Importance of the secondary vegetation sink, Global Biogeochem. Cycles, 23(2), GB2022, doi:10.1029/2007GB003176, 2009.

Stocker, B. D. and Joos, F.: Quantifying differences in land use emission estimates implied by definition discrepancies, Earth Syst. Dynam., 6(2), 731–744, doi:10.5194/esd-6-731-2015, 2015.

Stocker, B. D., Feissli, F., Strassmann, K. M., Spahni, R. and Joos, F.: Past and future carbon fluxes from land use change, shifting cultivation and wood harvest, Tellus B, 66(0), doi:10.3402/tellusb.v66.23188, 2014.

778 van der Werf, G. R., Randerson, J. T., Giglio, L., Collatz, G. J., Mu, M., Kasibhatla, P. S., Morton, D. C.,
779 DeFries, R. S., Jin, Y. and van Leeuwen, T. T.: Global fire emissions and the contribution of
780 deforestation, savanna, forest, agricultural, and peat fires (1997–2009), Atmos. Chem. Phys., 10(23),
781 11707–11735, doi:10.5194/acp-10-11707-2010, 2010.

782 Wilkenskjeld, S., Kloster, S., Pongratz, J., Raddatz, T. and Reick, C. H.: Comparing the influence of net
783 and gross anthropogenic land-use and land-cover changes on the carbon cycle in the MPI-ESM,
784 Biogeosciences, 11(17), 4817–4828, doi:10.5194/bg-11-4817-2014, 2014.

785 Yang, X., Richardson, T. K. and Jain, A. K.: Contributions of secondary forest and nitrogen dynamics to
786 terrestrial carbon uptake, Biogeosciences, 7(10), 3041–3050, doi:10.5194/bg-7-3041-2010, 2010.

787 Yue, C., Ciais, P., Cadule, P., Thonicke, K., Archibald, S., Poulter, B., Hao, W. M., Hantson, S.,
788 Mouillot, F., Friedlingstein, P., Maignan, F. and Viovy, N.: Modelling the role of fires in the terrestrial
789 carbon balance by incorporating SPITFIRE into the global vegetation model ORCHIDEE – Part 1:
790 simulating historical global burned area and fire regimes, Geosci. Model Dev., 7(6), 2747–2767,
791 doi:10.5194/gmd-7-2747-2014, 2014.

792 Yue, C., Ciais, P., Luyssaert, S., Li, W., McGrath, M. J., Chang, J. and Peng, S.: Representing
793 anthropogenic gross land use change, wood harvest and forest age dynamics in a global vegetation model
794 ORCHIDEE-MICT (r4259), Geosci. Model Dev. Discuss., 2017, 1–38, doi:10.5194/gmd-2017-118,
795 2017.

796

797 **Data availability**

798 All data used to generate the figures are available in the Supplement of this paper.

799

800 **Competing interests**

801 The authors declare that they have no conflict of interest.

802

803 **Acknowledgments**

804 We thank Dr. Benjamin D. Stocker for the constructive comments on an earlier version of this manuscript.
805 C.Y., P.C. and W.L. acknowledge support from the European Research Council through Synergy grant
806 ERC-2013-SyG-610028 “IMBALANCE-P”. W.L. and C.Y. are also supported by the European
807 Commission-funded project LUC4C (No. 603542).

808

Biogeosciences Discuss., https://doi.org/10.5194/bg-2017-329
Manuscript under review for journal Biogeosciences
Discussion started: 4 September 2017

Tables and figures

Table 1 Factorial simulations to quantify E_{LUC} from each of the LUC processes considered: net land use change ($E_{LUC\ net}$), land turnover ($E_{LUC\ turnover}$) and wood harvest ($E_{LUC\ harvest}$), with $E_{LUC\ all}$ being carbon emissions from all the three processes. The plus sign ("+") indicate that the process in question is included, with $S0_{ageless}$ ($S0_{age}$) having no LUC activities to $S3_{ageless}$ ($S3_{age}$) including all LUC processes. E_{LUC} is quantified as the difference in net biome production (NBP) between simulations without and with LUC.

Simulations and LUC processes included			
Simulations	Net land use change	Land turnover	Wood harvest
$S0_{ageless}$ ($S0_{age}$)			
$S1_{ageless}$ ($S1_{age}$)	+		
$S2_{ageless}$ ($S2_{age}$)	+	+	
$S3_{ageless}$ ($S3_{age}$)	+	+	+
Calculation of E_{LUC}			
No age dynamics ($S_{ageless}$)		With age dynamics (S_{age})	
$E_{LUC\ net,\ ageless} = NBP_{S0,\ ageless} - NBP_{S1,\ ageless}$		$E_{LUC\ net,\ age} = NBP_{S0,\ age} - NBP_{S1,\ age}$	
$E_{LUC\ turnover,\ ageless} = NBP_{S1,\ ageless} - NBP_{S2,\ ageless}$		$E_{LUC\ turnover,\ age} = NBP_{S1,\ age} - NBP_{S2,\ age}$	
$E_{LUC\ harvest,\ ageless} = NBP_{S2,\ ageless} - NBP_{S3,\ ageless}$		$E_{LUC\ harvest,\ age} = NBP_{S2,\ age} - NBP_{S3,\ age}$	
$E_{LUC\ all,\ ageless} = NBP_{S0,\ ageless} - NBP_{S3,\ ageless}$		$E_{LUC\ all,\ age} = NBP_{S0,\ age} - NBP_{S3,\ age}$	

Biogeosciences Discuss., https://doi.org/10.5194/bg-2017-329
Manuscript under review for journal Biogeosciences
Discussion started: 4 September 2017

Table 2 Determination of woody biomass thresholds for different age classes of forest PFTs. The thresholds of woody biomass for the first three age classes are determined by looking up via the biomass-age curve (Eq. 2), the ratio of woody biomass to the maximum biomass (B_{max}) that correspond to certain ages (years), followed by multiplying this ratio with equilibrium biomass (B_{max}) at each grid cell. Numbers within parentheses indicate the ratio of woody biomass to the maximum woody biomass (B_{max} in Eq. 2).

	Tropical forest (PFT 2, 3)	Temperate forest (PFT 3, 4, 5)	Boreal forest (PFT 6, 7, 8)
Age1	3 year (0.1)	3 year (0.07)	3 year (0.04)
Age2	9 year (0.26)	10 year (0.22)	15 year (0.19)
Age3	15 year (0.39)	20 year (0.40)	30 year (0.34)
Age4	0.6 × B_{max}		
Age5	0.8 × B_{max}		
Age6	1.2 × B_{max}		

Table 3 Carbon emissions from gross and net land use transitions, contributions of gross transitions to the total emissions from different studies, adapted from Hansis et al. (2015).

Reference	Time period	E_{LUC} (Pg C)			Contribution of gross transitions, Pg C (%)
		Gross transitions	Net transitions		
This study (With age dynamics)	1850-2005	147		99	22(15%)
This study (No age dynamics)	1850-2005	158		104	31(20%)
Hansis et al (2015)	1500–2012	382	secondary land only	374	8.5 (2%)
Hansis et al (2015)	1500–2012	382	primary land first	290	92.4 (24%)
Hansis et al (2015)	1500–2012	382	primary land last	296	85.8 (22%)
Stocker et al (2014)	1850–2004	171		146	25 (15%)
Wilkenskjeld et al (2014)	1850–2005	225		140	85 (38%)
Houghton (2010)	1850–2005	156			(28%, tropics)

[a]The last column gives the difference between the net LULCC flux estimates for gross and net transitions (absolute in Pg C and relative to the net LULCC flux for gross transitions).

Biogeosciences Discuss., https://doi.org/10.5194/bg-2017-329
Manuscript under review for journal Biogeosciences
Discussion started: 4 September 2017

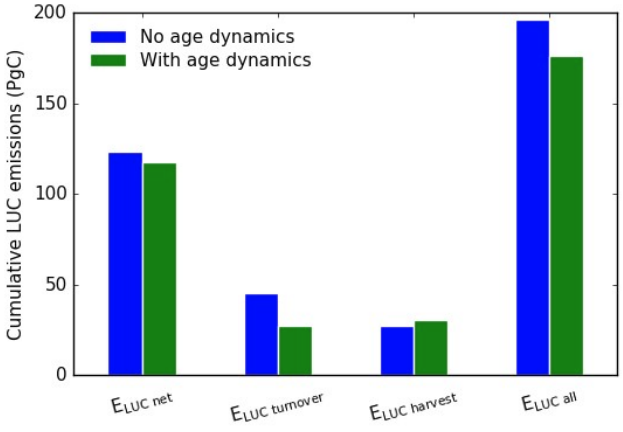

Fig. 1 Global cumulative land use change carbon missions for 1501–2005.

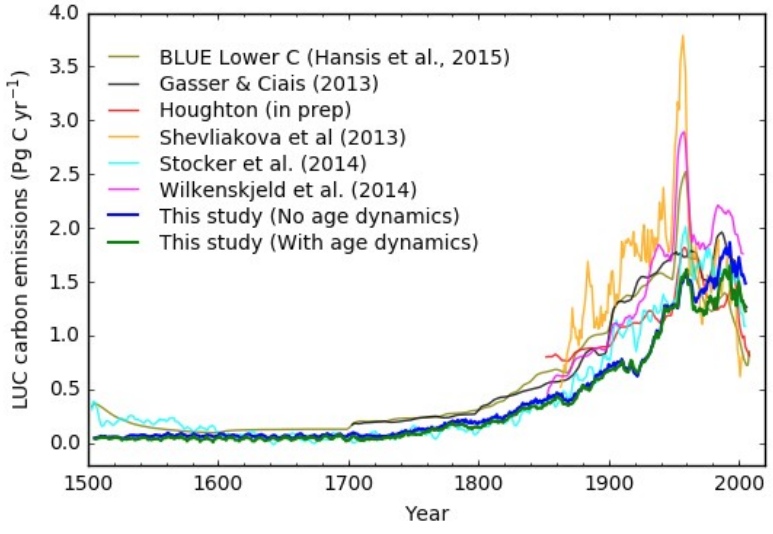

Fig. 2 Annual carbon emissions from historical land use change over the globe by our studies and from other previous studies. Results of this study are smoothed using a ten-year average moving window; data of other studies are from Figure 5 Hansis et al (2015) and are smoothed using a five-year moving average window.

Biogeosciences Discuss., https://doi.org/10.5194/bg-2017-329
Manuscript under review for journal Biogeosciences
Discussion started: 4 September 2017

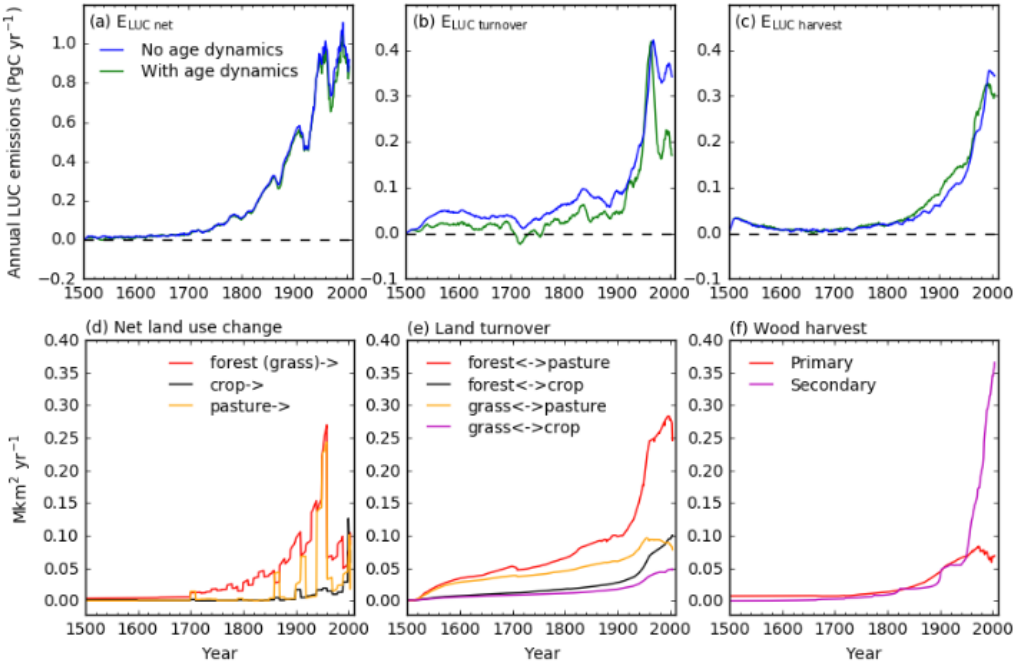

Fig. 3 Upper panels: annual carbon emissions since 1501 from different LUC processes, (a) net land use change, (b) land turnover and (c) wood harvest. Data are smoothed using a ten-year average moving window. Lower panels: annual time series of areas impacted by different LUC processes. (d) Area losses of forest, grassland, cropland and pasture as a result of net land use change. Note that we assume equal contributions by forest and grassland to agricultural land when backcasting historical land cover maps and net land use transitions, thus area losses of forest and grassland are identical. (e) Areas subject to land turnover. (f) Areas of wood harvest from primary and secondary forests.

Biogeosciences Discuss., https://doi.org/10.5194/bg-2017-329
Manuscript under review for journal Biogeosciences
Discussion started: 4 September 2017

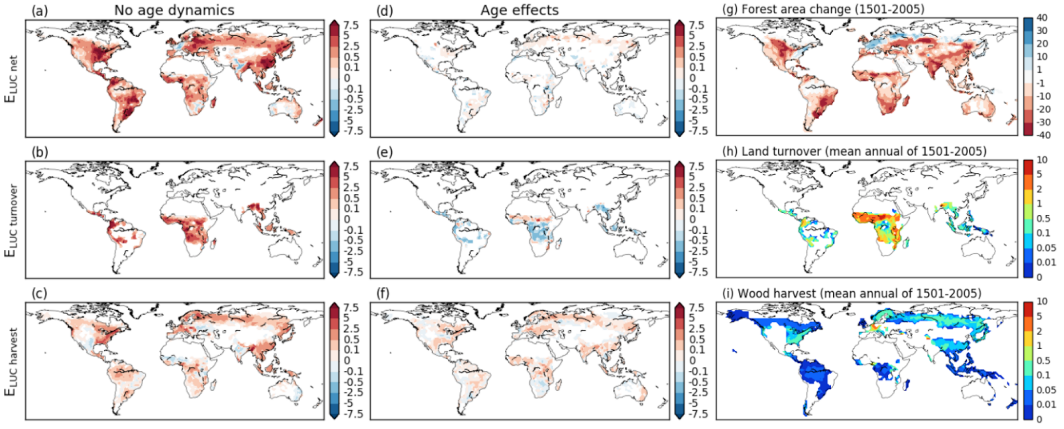

Fig. 4 (a)-(c): Spatial distribution of E_{LUC} from different LUC processes by the simulation without sub-grid age dynamics for 1501-2005 in unit of kg C m^{-2}, for (a) net land use change, (b) land turnover and (c) wood harvest. Subplots (d)–(e) show the age effect as the difference between $E_{LUC\ age}$ and $E_{LUC\ ageless}$ for each LUC process, with positive (negative) values indicating higher (lower) E_{LUC} by the S_{age} simulation. (g) Cumulative forest loss as a result of net land use change for 1501–2005 as a percentage of grid cell area. (h) Mean annual grid cell percentage impacted by land turnover over1501–2005. (i) Mean annual grid cell percentage impacted by wood harvest (i.e., sum of wood harvest on primary and secondary forests) over 1501–2005.

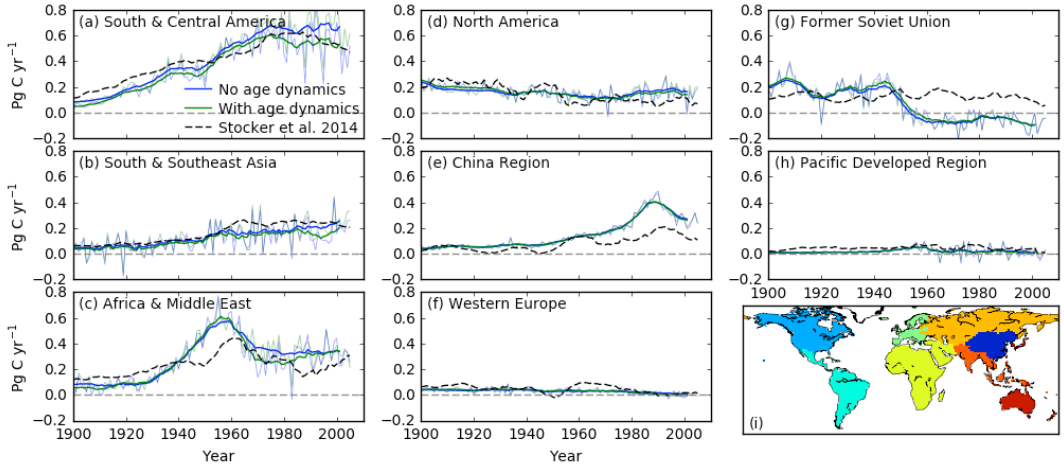

Fig. 5 (a)-(h) Temporal pattern of regional land use change emissions in comparison with those from Stocker et al. (2014). Thicker solid lines indicate smoothed annual emissions by ten-year moving average

Biogeosciences Discuss., https://doi.org/10.5194/bg-2017-329
Manuscript under review for journal Biogeosciences
Discussion started: 4 September 2017

from our study, with blue (green) showing emissions from $S_{ageless}$ (S_{age}) simulations. Thinner solid lines indicate unsmoothed annual emissions from our study. Gray dashed lines indicate estimations from Stocker et al. (2014), smoothed by ten-year moving average. Regional segregation of the globe is shown in the subplot (i).

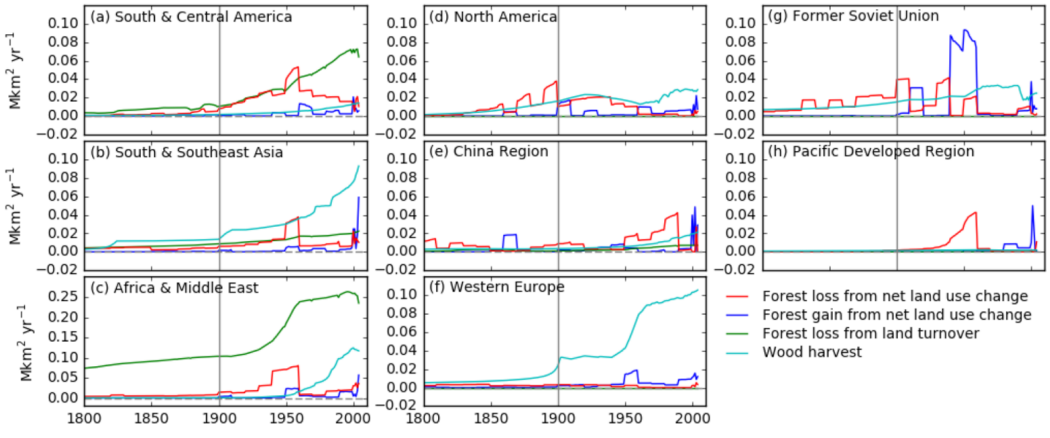

Fig. 6 Annual regional areas subject to land use change. Only land use change activities involving forests are assumed to have dominant impacts on land use change emissions and are thus shown here: forest loss (red line) and gain (blue line) from net land use change, occurring within the same region but not in the same model grid cell; forest in involved in land turnover (green line) and wood harvest (cyan line), where forested land remain a forest after land use change. Note that the scale of y-axis is the subplot (c) is different from the others. See Fig. 5 for the spatial extents of different regions.